Journal of Fluids and Structures 17 (2003) 1059–1078

JOURNAL OF FLUIDS AND STRUCTURES

www.elsevier.nl/locate/jnlabr/yjfls

Interference effect of an upstream larger cylinder on the lock-in vibration of a flexibly mounted circular cylinder

K.M. Lam*, A.P. To[1]

Department of Civil Engineering, The University of Hong Kong, Pokfulam Road, Hong Kong, China

Received 30 September 2002; accepted 25 March 2003

Abstract

Experiments have been carried out to investigate the flow-induced vibration response of a flexibly mounted circular cylinder located in the vicinity of a larger cylinder and subjected to cross-flow. The interfering larger cylinder was placed upstream and had a diameter twice that of the vibrating cylinder. Complex interaction was observed between the flow over the two cylinders. The vibration responses of the flexible cylinder were classified into different regimes according to the relative positions of the two cylinders. In the-side-by-side arrangement and the tandem or near-tandem arrangement, flow-induced vibrations of the flexible cylinder were greatly suppressed. In the staggered arrangement which covered a large portion of the relative cylinder positions being investigated, vibrations of the smaller cylinder were greatly amplified. The vibration response curves were also largely modified with a broadening of the lock-in resonance range. A shift of the peak reduced velocity for maximum vibration response was also found. Flow visualizations and wake velocity measurements suggested that the modifications of the vibration responses were related to the presence or absence of constant or intermittent flow through the gap region between the two cylinders. The proposed mechanisms of flow interactions and the resulting vibration response characteristics could explain previous observations on flow-induced vibrations of two equal-sized circular cylinders reported in the literature.

1. Introduction

Flow-induced vibrations of elongated bluff bodies have attracted a lot of attentions from the perspectives of basic fluid dynamics and engineering applications. There have been many review papers on the topic, in particular on the flow-induced vibrations of a circular cylinder in cross-flow (e.g., Sarpkaya, 1979; Bearman, 1984; Griffin and Hall, 1995). For a long flexible circular cylinder or a circular cylinder elastically mounted, the lock-in phenomenon with the associated vibration is probably the most widely studied problem of fluid–structure interaction. For an isolated cylinder in a uniform and smooth cross-flow, large amplitude "lock-in" vibration of the cylinder occurs when the vortex shedding frequency is near to the natural frequency of cylinder vibration (Blevins, 1994). In addition, the vortex shedding frequency becomes "locked-on" to the natural frequency and does not follow the change in freestream velocity.

According to the monograph of Naudascher and Rockwell (1994), excitation sources of flow-induced vibration can be classified into three types of mechanism. They are "instability-induced excitation" (IIE), "movement-induced excitation" (MIE), and "extraneously induced excitation" (EIE). The lock-in vibration is an example of IIE and the "lock-on" of shedding frequency may be classified under MIE. IIE originates from an instability of the flow itself.

*Corresponding author. Tel.: +852-2859-1975; fax: +852-2559-5337.
E-mail address: kmlam@hku.hk (K.M. Lam).
[1] Now with Ove Arup & Partners (Hong Kong) Limited, 5/F, Festival Walk, Tat Chee Avenue, Kowloon Tong, Hong Kong, China.

0889-9746/03/$ - see front matter © 2003 Published by Elsevier Science Ltd.
doi:10.1016/S0889-9746(03)00065-3

Alternating vortex shedding from a circular cylinder and the resulting periodically fluctuating fluid forces are an example of IIE. The lock-in vibration of a flexible or flexibly mounted cylinder is sustained by the periodic fluctuating lift force whose frequency coincides with the natural frequency of cylinder vibration. Lock-in vibration is thus brought about by IIE. MIE is due to fluctuating fluid forces which are linked to movements of the vibrating body in a flow. In lock-in vibration, the cylinder vibrates in the flow with significant-level amplitudes at its natural frequency of vibration. The cylinder movement disturbs the natural instability associated with vortex shedding. The actual vortex shedding frequency becomes locked-on to the frequency of cylinder movement as a result of MIE. Thus, both IIE and MIE are present in lock-in vibration.

The third source of excitation, EIE, is caused by fluctuations in flow velocity or pressure which are independent of the flow instability originating from the cylinder and independent on the cylinder movements. Turbulence buffeting is a common example in which fluctuating fluid forces are produced on a body due to turbulence in the incoming flow. In cylinder vibrations, lock-on resonance of the shedding frequency under EIE has been achieved on a fixed circular cylinder by imposing a large-amplitude periodic fluctuating component on the incident freestream flow (e.g., Barbi et al., 1986; Armstrong et al., 1987). Another common experimental technique to achieve the same excitation mechanism is to oscillate a cylinder in-line with a smooth uniform flow (e.g., Griffin and Ramberg, 1976). Provided the cylinder diameter is small compared to the acoustic wavelength, the two situations are completely equivalent to an observer moving with either the cylinder or the freestream. For these in-line oscillations, the most intense lock-on occurs when the frequency of oscillation, either of the cylinder or of the flow, is near to the frequency of the fluctuating drag forces due to natural vortex shedding, which is twice the natural vortex shedding frequency. Lock-on of vortex shedding can also be made to occur by oscillating a fixed cylinder in the cross-flow direction (e.g., Ongoren and Rockwell, 1988). In this lift direction, vortex resonance occurs when the excitation frequency is near to the natural vortex shedding frequency which is the frequency of the fluctuating lift. For both in-line and cross-flow vibrations, some forms of resonance are observed in the sub-harmonic and harmonic frequencies in addition to the fundamental lock-on frequency.

When a flexible cylinder is placed in the vicinity of another cylinder, the flow field incident on it consists of coherent fluctuations induced by the flow over the neighbouring cylinder. Modification of lock-in vibration can occur as a result of the "extraneously induced excitation" caused by the interfering cylinder. Most of this kind of studies have been focused on two equal-sized cylinders (e.g., Tanida et al., 1973; King and Johns, 1976; Bokaian and Geoola, 1984). It is generally observed that in the wake of an upstream cylinder, a flexible cylinder undergoes cross-flow vibrations over a wider range of reduced velocity. In this paper, an experimental investigation of the cross-flow vibration characteristics of a flexibly mounted circular cylinder under different reduced velocities will be reported. The cylinder is under the influence of a neighbouring larger stationary cylinder with a diameter twice in size. This situation is representative of full-scale structural engineering application where a slender and more flexible cylinder-like structure such as a tall chimney is erected near a larger and more rigid structure. On the fundamental side, the situation is different from that of two equal-sized cylinders. The "extraneously induced excitation" due to a larger upstream cylinder is expected to be of a higher level and there is a fixed ratio of two between the natural shedding frequencies from the two cylinders.

2. Experimental techniques

The experiments were carried out in a wind tunnel with an octagonal test section of width 44 cm. Uniformity of wind profiles across the middle 90% of the test section had been checked within 1% of the mean velocity. The turbulence intensity was below 0.01. Two aluminium cylinders of diameters $D = 3.2$ cm and $d = 1.6$ cm were mounted horizontally in the test section. Two square end plates of size 30 cm were installed. Uniform two-dimensional smooth flow around the cylinders was provided in the 32 cm wide section between the end plates. The effective length-to-diameter aspect ratios were 10 and 20 for the two cylinders.

Both cylinders were structurally rigid along the length. The larger cylinder was firmly mounted at both ends into the wind tunnel walls and there was no detectable free vibrations or flow-induced vibration on it. The smaller cylinder was mounted elastically in order to investigate its flow-induced vibration characteristics. It was suspended across the middle of the test section with two piano wires. There were holes of small but enough clearance in the end plates to allow the cylinder to undergo vibrations. Drag wires were installed to the cylinder to restrict in-line movement. The natural frequency of the coherent vertical cross-flow vibration of the cylinder under the present suspension system could be tuned by varying the tension in the piano wires. It was set at a fixed value of $f_n = 10.5$ Hz during all the experiments. A low value of reduced damping was required to achieve high amplitude lock-in and this was provided by the use of thin-walled hollow aluminium tube for the cylinder and the piano wires for suspension. A value of about 0.002 was obtained for the damping ratio from a free vibration test.

The range of reduced velocities under investigation was roughly from $U_R = U/f_n d = 4$ to $U_R = 20$, U being the freestream velocity. The Reynolds number based on the small cylinder diameter varied from Re = 720 to Re = 3600.

It has been reported that the natural frequencies of vibration of a combined fluid–cylinder system in flow-induced vibration experience a rather sudden variation in values near resonance (Zhou et al., 2001). The observations were reported on a long cylinder, aspect ratio above 50, with fixed support at both ends. The flow-induced vibration was along the length of that cylinder and the reported variations in first-mode frequencies were at most $\pm 5\%$. In the present study, the cylinders were shorter in aspect ratio and much more rigid along their lengths. The natural frequency of the rigidly mounted larger cylinder measured with an accelerometer was above 250 Hz. The reduced velocities based on the larger cylinder were below 0.4 in all the tests and far from resonance. The frequency at which the flexibly mounted smaller cylinder vibrated in each test was measured from spectral analysis of the vibration signal. In all situations where significant levels of flow-induced vibration occurred, negligible differences were found between the actual frequency of vibration and the static value of 10.5 Hz. The effects of possible variations in natural frequencies of the two cylinders near resonance were thus not considered.

Observations during the experiments had shown that with the suspension method, the smaller cylinder exhibited pure cross-flow vibration in the vertical direction at reduced velocities from zero up to values around 15. The up-and-down movements across the span of the cylinder were highly in phase. It was only at reduced velocities above 18 that out-of-phase vibration came in and a torsional vibration mode was observed in addition to the up-and-down vibration. More details will be given later.

A series of experiments were carried out with the interfering larger cylinder placed in 64 different locations around the flexibly mounted cylinder. The relative positions between the two cylinders were given with reference to the larger cylinder. The separation X_0 and Y_0 denote the position of the central axis of the small cylinder as measured respectively downstream and laterally from the central axis of the larger cylinder. The 64 cylinder arrangements covering the range of $0 \leqslant X_0/D \leqslant 2.34$ and $0 \leqslant Y_0/D \leqslant 1.41$ are shown schematically in Fig. 1. The letter in each arrangement position denotes the classification scheme to be described later.

At each arrangement of the two cylinders, the vibration signal of the small cylinder was measured with a non-contact displacement sensor at a number of different freestream velocities in the wind tunnel. After a change in velocity, the small cylinder was given an initial lateral displacement of about $0.5d$ to enhance a faster establishment of flow-induced vibration. Then the vibrating signal was recorded in a data-acquisition computer for 30 s in every minute. The root-mean-square (r.m.s.) amplitude of the vibrations in every 30-s sampling period was calculated inside the computer. When the r.m.s. amplitudes in two consecutive periods were close to within 0.5% of each other, the force-induced vibration was considered to be fully established to its steady-state. The vibration signal was then stored into the

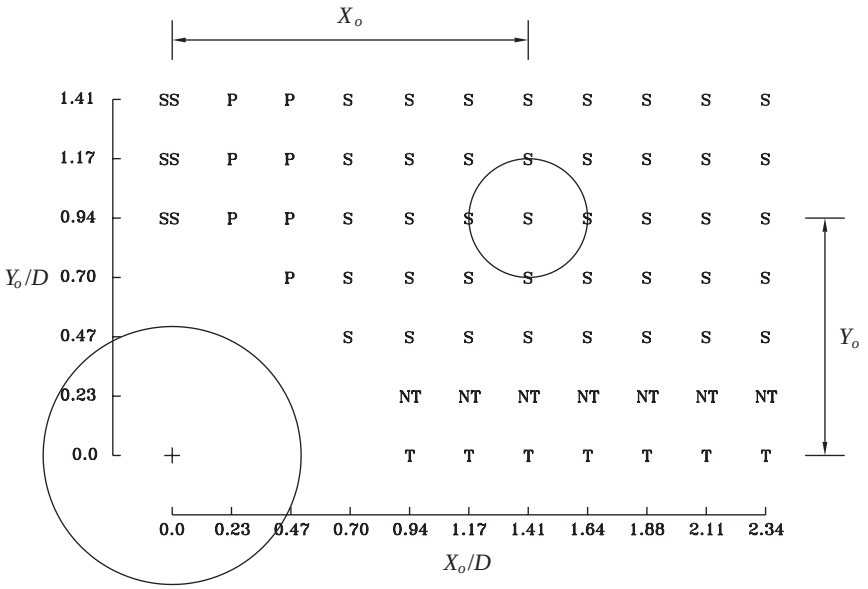

Fig. 1. Arrangement positions of the two cylinders in the experiments. T—Tandem, NT—Near-tandem; SS—Side-by-side; P—Proximity; and S—Staggered.

computer for subsequent analysis. The vibration response of the flexible cylinder was shown by plotting the r.m.s. vibration amplitude, $y_{\text{r.m.s.}}$ against the reduced velocity U_R.

Flow visualizations were carried out to investigate the vortex interaction. A smoke wire was placed in the vertical direction upstream of the two cylinders. A commercial fog fluid (from Dantec/Invent) was used and the evaporated fog droplets of diameters less than 6 μm formed a dense white fog. The fog pattern flowing around the cylinder was visualized with a laser sheet which cut through a longitudinal vertical section in the wind tunnel. A 3-W Argon-ion laser was used and a flat mirror was installed on the far-end to reflect the laser sheet so that illumination could be made to all sides of the cylinders. In order to capture the flow pattern at different positions of the vibrating small cylinder, a phase-locked technique was used. An electronically controlled laser shutter was placed between the laser tube and the laser sheet generator and it was connected to a circuitry which registered the vibrating signal of the small cylinder. At a preset phase of the cylinder vibration, say at one of its two extreme positions, the laser shutter was opened for a short time of 10 ms to allow laser illumination to the wind tunnel. The image was recorded in an image frame of a CCD camera which was captured digitally into a computer with a frame grabber (Data Translation DT2853). Each digital image had a resolution of 512 pixels × 512 pixels × 256 grey levels. The time of firing of the laser shutter was checked by comparing the signal from a photocell with the cylinder vibration signal so that a correct phase locking could be ensured. About 20 images were taken at a particular phase of cylinder vibration under a particular reduced velocity. It was observed that at reduced velocities where resonance did not occur and the vibration amplitude was low, the images did not show a repetitive pattern although they were captured at the same phase of cylinder movement. When resonance or lock-in vibration occurred, a highly repetitive pattern could be found among the images. This means that at resonance, the flow patterns, and hence the fluid forces, are highly synchronized with the cylinder movement.

Some velocity measurements were made in the wake of the two cylinders. Only the streamwise velocity component was measured with a single hot wire. The small cylinder was kept stationary during the measurement and a fixed freestream velocity at 5.5 m/s was used. The single hot wire measurements were intended to provide a crude idea of the flow around the cylinders and in particular, through the gap between the cylinders. The velocities in those regions were expected to be highly turbulent and having a mean flow direction at a large oblique angle to the freestream.

3. Results and discussion

3.1. Lock-in of the flexible cylinder alone

The vibration response of the flexible cylinder alone without the large cylinder in place has been obtained first. Fig. 2 shows the r.m.s. vibration amplitude at different reduced velocities. Lock-in resonance is observed to occur at reduced velocities from $U_R = 5$ to $U_R = 8$. The maximum vibration amplitude occurs at $U_R = 6.1$ and the r.m.s. amplitude is $y_{\text{r.m.s.}}/d = 0.085$. While the peak-to-peak amplitude is usually reported in the literature, lock-in vibration in the present study is observed to occur in a near perfectly sinusoidal manner. As the peak amplitude can be related to the r.m.s. amplitude, it is decided to use the more statistically confident r.m.s. amplitude for presentation. In Fig. 2, another parameter, the frequency ratio f_s/f_n, is given on the horizontal velocity axis. The value f_s is the vortex shedding frequency from the small cylinder at the particular velocity if it is free from flow-induced vibration and interference from other bodies. By Strouhal similarity, f_s is linear proportional to U and can thus be used to denote the velocity

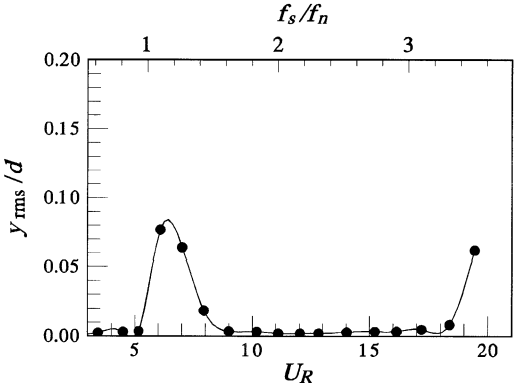

Fig. 2. Vibration response of the flexible cylinder alone.

change. The frequency ratio has been commonly used to describe the lock-on phenomenon in studies on oscillating cylinders (e.g., Griffin and Hall, 1995). In Fig. 2, the maximum amplitude vibration occurs at $f_s/f_n = 1.1$. The lock-in response is typical and consistent with results of previous studies reported in the literature (Blevins, 1994; Naudascher and Rockwell, 1994).

Outside the lock-in range, vibrations at very small amplitude are observed until U_R reaches 18. At higher velocities, the amplitude of vibrations increases. The vibration is not of the pure up-and-down mode but includes a significant torsional mode. The vertical movements of the two ends of the cylinder are out-of-phase and a spectral analysis of the vibration signal reveals two dominant frequency components. One is the coherent up-and-down mode at 10.5 Hz and the other is at 12.2 Hz which is related to the natural frequency for the torsional mode.

Some phase-locked smoke patterns are shown in Fig. 3. The most severe lock-in resonance occurs at $U_R = 6.1$. At this velocity, highly repetitive smoke patterns are observed at the same phase among different cycles of the cylinder vibration. When the cylinder is at the uppermost position of its vibration in the figure (Fig. 3a), fluid from the freestream is observed to flow around the upper side of the cylinder into the wake region forming a recirculating vortex. Farther downstream, fluid previously entrained into the wake from the lower side of the cylinder becomes a shed vortex. When the cylinder is at its lowermost position, the flow pattern observed in Fig. 3b is exactly the up-and-down mirror image of Fig. 3a. This phase relation between the vortex pattern and the cylinder movement during lock-in resonance has been observed in past studies (e.g., Ongoren and Rockwell, 1988). At a slightly lower reduced velocity, at $U_R = 5.2$, the same phase relationship is observed between the vortex pattern and the cylinder vibration position but the vortex formation length is much shorter (Fig. 3c). The "vortex formation length" can be taken as the longitudinal distance from the cylinder centre to the first saddle point in the smoke trace. Fig. 3d shows an example of phase-locked vortex patterns at $U_R = 7.0$. This reduced velocity is slightly higher than the lock-in resonance value. It has been found in the literature that when the reduced velocity increases beyond the lock-in resonance value, an 180° phase shift in the vortex pattern occurs. Most of the previous studies (e.g., Ongoren and Rockwell, 1988) are based on the forced vibration method and there seems no recorded observation of phase shift in free vibration studies. In the present study, the phase-locked smoke images are found to exhibit two patterns. One pattern is shown in Fig. 3d where there is a phase shift from the pattern in Fig. 3b. For some of the time, there is another pattern with the same phase relationship as that at the lower reduced velocities. More details can be found in To (1998).

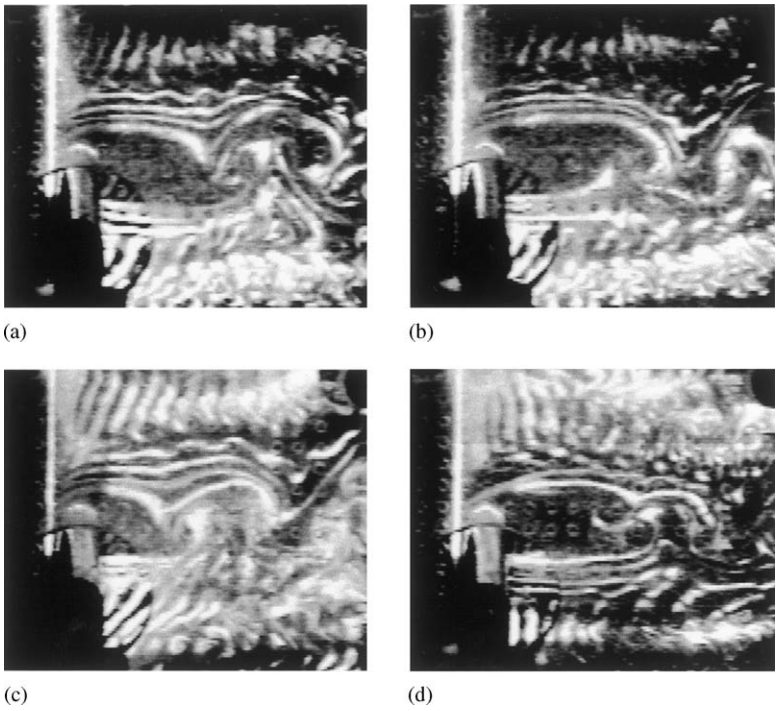

Fig. 3. Phase-locked smoke pictures of the isolated flexible cylinder. (a) $U_R = 6.1$, cylinder at upper extreme position; (b) $U_R = 6.1$, cylinder at lower extreme position; (c) $U_R = 5.2$, cylinder at upper extreme position; (d) $U_R = 7.0$, cylinder at lower extreme position.

3.2. Interference effect due to the larger cylinder

When the larger cylinder is placed in the neighbourhood of the flexible cylinder, the vibration response of the latter is largely affected. Fig. 4 shows an overview of the modified response curves of the flexible cylinder at the 64 cylinder positions. According to the general pattern of the response curves, the 64 cylinders positions are classified into different arrangement regimes. The regimes have been shown in Fig. 1 and the abbreviations for the cylinder arrangement types are: Tandem (T); Near-Tandem (NT); Side-by-Side (SS); Proximity (P); and Staggered (S). In the tandem, near-tandem and side-by-side arrangements, vibration amplitudes of the flexible cylinder are greatly reduced by the presence of the larger cylinder. In most of the proximity arrangements, peak vibration levels of the flexible cylinder occur at roughly the same reduced velocity as the isolated cylinder situation. In the staggered arrangements, large-amplitude vibrations of the flexible cylinder occur at a wider range of reduced velocities and the reduced velocity of maximum lock-in response shifts significantly away from that of the isolated cylinder situation.

3.3. Tandem and near-tandem arrangement

When $Y_0/D = 0$ or 0.23, the smaller flexible cylinder is shielded completely by the upstream larger cylinder. The vibration amplitudes are negligibly small at all reduced velocities. Examples of two response curves at $(X_0/D, Y_0/D) = (1.41, 0.23)$ and (2.34, 0) are shown in Figs. 5a and b. The response curve in the isolated cylinder situation is shown in broken line for comparison. In these and later figures showing vibration response curves, the r.m.s. vibration amplitude of the flexible cylinder is shown on a relative scale to the peak r.m.s. amplitude of the cylinder in its isolated situation at lock-in resonance. This peak amplitude, $y_{\text{r.m.s.(peak, isolated)}}$ has been found to have a value of $0.085d$ (Fig. 2).

Being immersed in the wake of the larger cylinder, the flexible cylinder is deprived of its natural vortex shedding and lock-in vibration is prohibited. Fig. 6 shows an example of single wire velocity measurement in the region around the flexible cylinder. The profiles of mean and r.m.s. axial velocities clearly reveal the shielding effect offered by the larger cylinder. Because of the negligible amplitude of cylinder vibration, flow visualization pictures phase-locked to the cylinder movement could not be obtained. Randomly captured pictures show that no distinct vortices are shed from the smaller cylinder. Regular vortex shedding is, however, observed on the larger cylinder.

The present response characteristics are very different from those made on two equal-sized cylinders (Bokaian and Geoola, 1984) in which the downstream cylinder was observed to undergo rigorous vibrations at $U_R = 6.0$. When the two cylinders are of the same size, the downstream cylinder is not completely blocked by the upstream cylinder and can develop its own vortex shedding. The vortex-induced fluctuating lift due to IIE is helped by the flow disturbance of the same frequency from the upstream cylinder. This results in enhanced lock-in vibration.

When the smaller cylinder is at a longer distance downstream from the larger cylinder, some obvious vibrations occur at $U_R = 12$ (Fig. 5b). This reduced velocity is about double that of the isolated cylinder situation (the frequency ratio f_s/f_n being 2.0 approximately). At this flow velocity, the natural vortex shedding frequency of the larger cylinder matches the natural frequency of vibration f_n of the flexible cylinder because of the 1:2 diameter ratio. Velocity spectra measured at locations behind the larger cylinder confirms that the incoming flow to the flexible cylinder contains fluctuations at f_n and thus excites the flexible cylinder to vibrate (To, 1998). The mechanism should be of the nature of EIE. The small amplitudes of vibrations, as compared with those in the lock-in of the isolated cylinder, suggest that there lacks a good correlation between the smaller cylinder movement and the vortex shedding from the upstream larger cylinder.

3.4. Side-by-side arrangement

When the larger cylinder is placed next to and close to the flexible cylinder at $X_0/D = 0$, no vibrations are observed throughout the whole velocity range being investigated (Fig. 4). When the lateral spacing between the cylinders increases to $Y_0/D = 1.41$, some lock-in vibration occurs around $U_R = 5.2$. This reduced velocity of peak response is lower than the value of 6.1 for the isolated cylinder. The peak amplitude of vibration is also much lower than that of the isolated cylinder situation. It is expected that the response of the flexible cylinder will return to that of the isolated cylinder situation as at Y_0/D increases further.

Fig. 7 shows the distribution of mean axial velocity at $Y_0/D = 1.17$. Flow through the gap region between the cylinders is strongly bent towards the rear of the smaller cylinder. This prohibits the normal development of a wake or a region of velocity deficit behind the smaller cylinder. This may explain the absence of any vibration at significant amplitudes over all reduced velocities.

The flow patterns at the larger lateral spacing of at $Y_0/D = 1.41$ is shown in Fig. 8. With sufficiently high amplitudes of vibration at $U_R = 5.2$, phase-locked visualizations can be made at this reduced velocity for this cylinder arrangement.

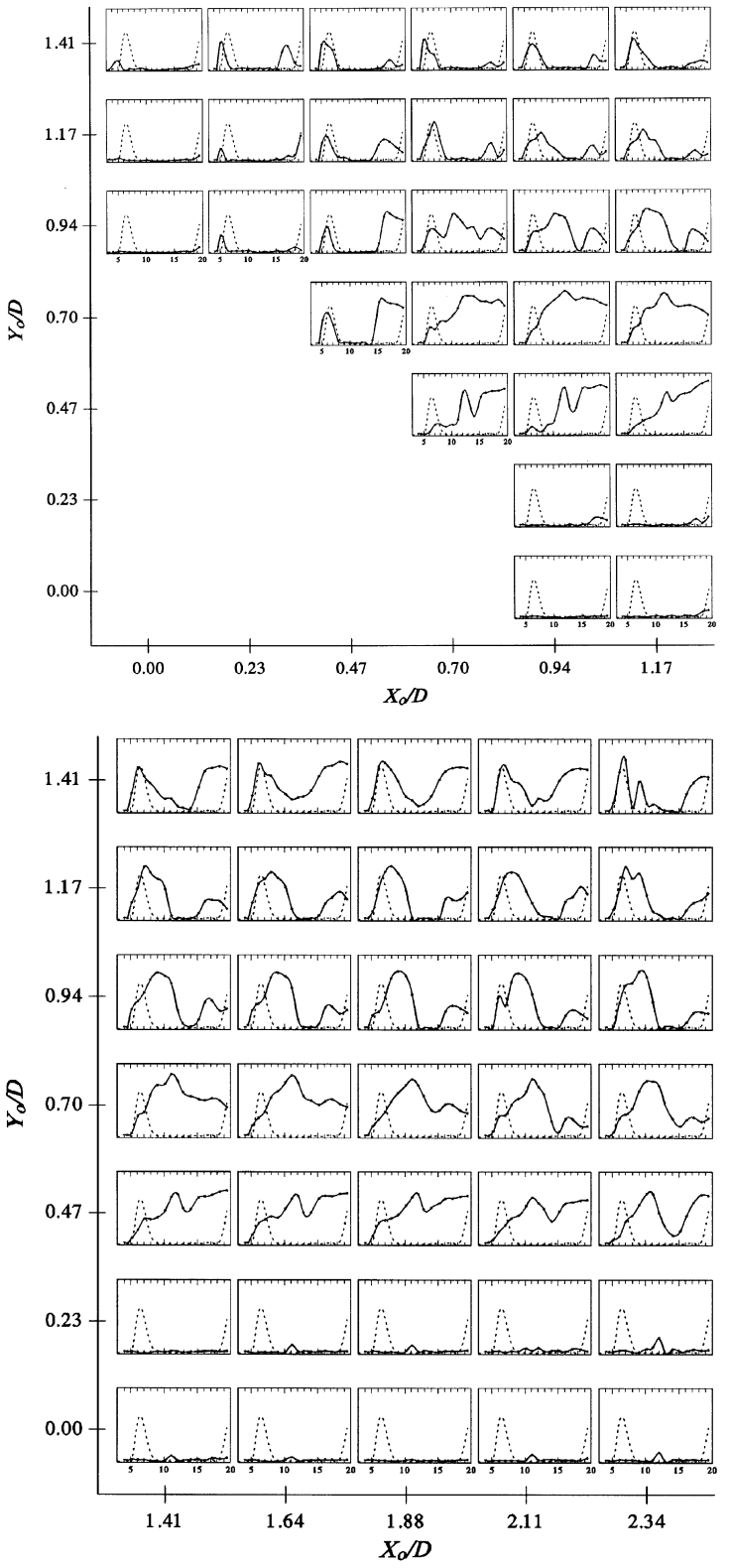

Fig. 4. Entire set of vibrating response curves of the flexible cylinder with the larger cylinder in the vicinity. The centre of each curve roughly represents the position of the smaller cylinder relative to the larger cylinder. The response curve of the isolated cylinder situation is shown in broken line. The horizontal axis of each curve is the reduced velocity U_R and the vertical axis is r.m.s. vibration amplitude.

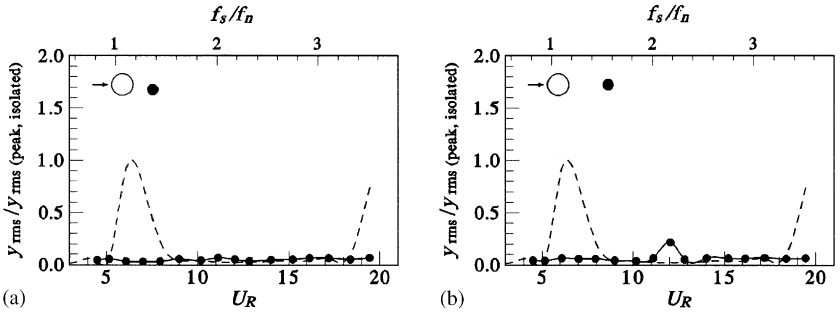

Fig. 5. Vibration response of the smaller cylinder in the tandem/near-tandem arrangement. (a) $(X_0/D, Y_0/D) = (1.41, 0.23)$; (b) $(X_0/D, Y_0/D) = (2.34, 0)$.

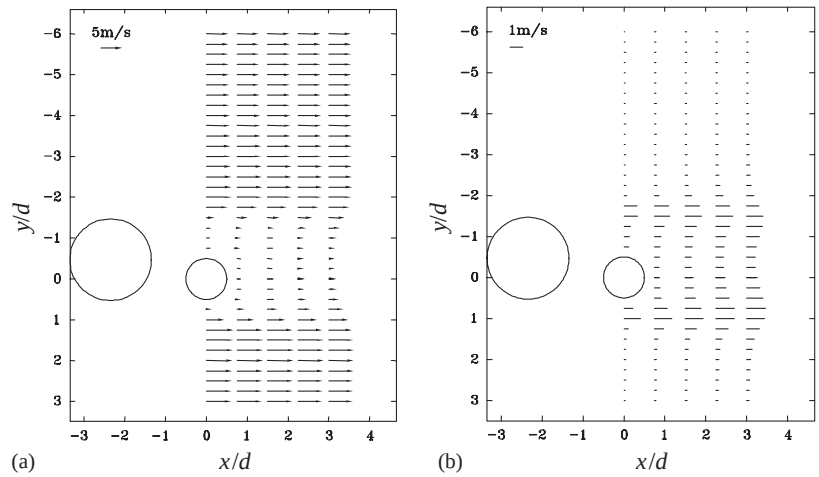

Fig. 6. Distribution of (a) mean axial velocity; and (b) r.m.s. velocity fluctuations in the wake of the two cylinders in the near-tandem arrangement $(X_0/D, Y_0/D) = (1.17, 0.23)$.

The smoke picture in Fig. 8a suggests evidence of vortex shedding from the smaller cylinder. It seems that as the gap between the two cylinders becomes wider, the degree of gap flow bending towards the smaller cylinder side is smaller. The mean axial velocity field in Fig. 8b shows the presence of a wake region behind the smaller cylinder which is better developed than that in Fig. 7. The bending of gap flow leads to a reduction in the wake width behind the smaller cylinder. The vortex shedding frequency is thus made higher and this may explain why lock-in occurs at a lower value of U_R. The excitation mechanism should be of the IIE type.

3.5. Proximity arrangement

The proximity arrangement covers the cylinder positions at $X_0/D = 0.23$ and 0.47. The smaller cylinder is slightly more downstream than the side-by-side arrangement. The cylinder undergoes vibration levels of the same order of magnitudes as in its isolated situation (Fig. 4). Fig. 9 shows again the vibration response curves at successive lateral separations at $X_0/D = 0.47$. There exists two resonance regions well separated from each other, one at reduced velocity around $U_R = 5.2$ and the other at $U_R > 14$. The first resonance region covers a reduced velocity range similar to the lock-in range of the isolated cylinder situation but the vibration amplitudes are smaller. For the second resonance region, it was observed during the experiments that the vibration was dominated by the torsional mode. Torsional vibration starts at $U_R > 14$ and the vibration amplitude increases sharply to a maximum near $U_R = 16$. At smaller lateral separations between the two cylinders, the torsional vibration retains large amplitudes with further increases in U_R. Similar response characteristics have been reported for two equal-sized cylinders (Bokaian and Geoola, 1984).

Fig. 10 shows an example of the mean axial velocity field around the two cylinders in the proximity arrangement. The separation between the cylinders is $(X_0/D, Y_0/D) = (0.47, 1.17)$. As contrary to the side-by-side arrangement in

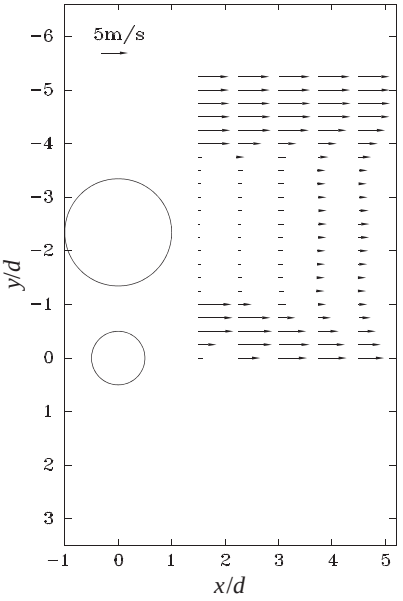

Fig. 7. Distribution of mean axial velocity in the wake of the two cylinders in the side-by-side arrangement $(X_0/D, Y_0/D) = (0, 1.17)$.

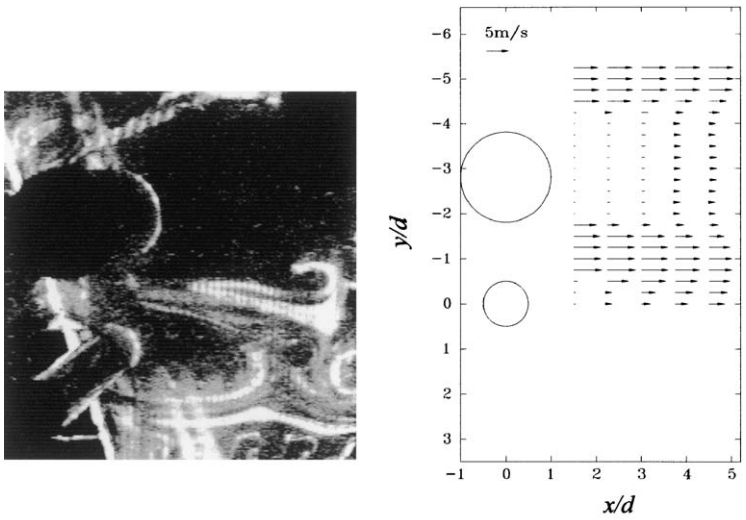

Fig. 8. Flow patterns in the farther side-by-side arrangement $(X_0/D, Y_0/D) = (0, 1.41)$. (a) Phase-locked smoke pictures at $U_R = 5.2$, smaller cylinder at extreme position farthest away from the larger cylinder. (b) Distribution of mean axial velocity in the wake.

Figs. 7 and 8, the flow in the gap region is bent towards the larger-sized cylinder wake. It appears that the flexible cylinder is partially shielded from the effect of the larger cylinder. Its vibration response thus retains the key features of the isolated cylinder situation. The peak response in the lock-in range, however, occurs at a slightly lower reduced velocity. This may be a result of the accelerated velocity in the gap region passing over the smaller cylinder. The excitation mechanism for the lock-in resonance is of the IIE type. The mechanism for the high-level torsional vibrations in the proximity arrangement remains to be explored.

It is evident from Fig. 4 that when the longitudinal separation increases beyond $X_0/D > 0.47$, the vibration responses changes to a completely different pattern (mainly noticeable at the smaller lateral separations). This is the next regime of cylinder arrangement referred to as the staggered arrangement.

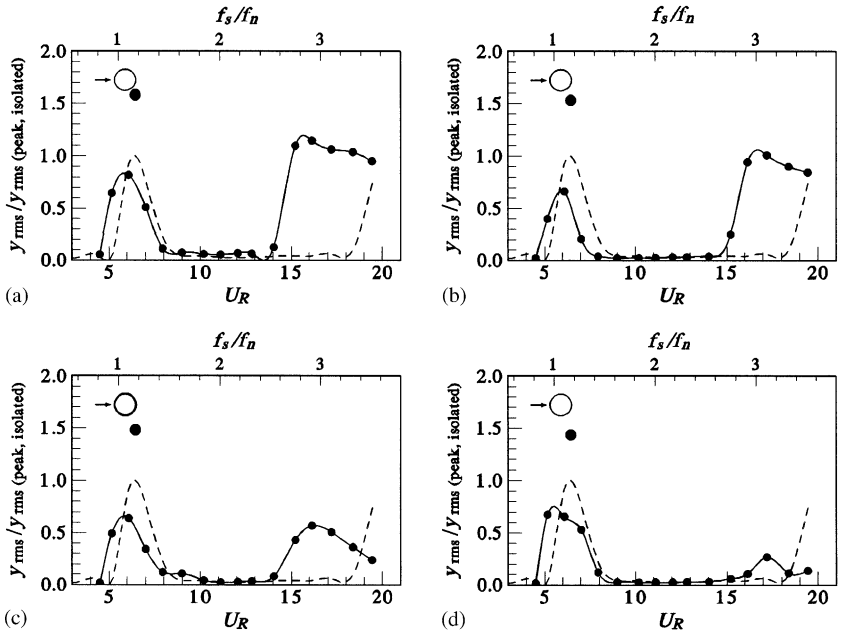

Fig. 9. Vibration response of the smaller cylinder in the proximity arrangement at $X_0/D = 0.47$. Y_0/D: (a) 0.70; (b) 0.94; (c) 1.17; (d) 1.41.

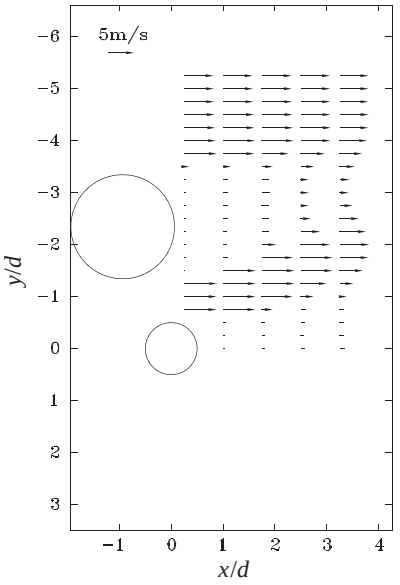

Fig. 10. Distribution of mean axial velocity in the wake of the two cylinders in the proximity arrangement $(X_0/D, Y_0/D) = (0.47, 1.17)$.

3.6. Staggered arrangement

The staggered cylinder arrangement covers the cylinder separations at $X_0/D \geqslant 0.70$ and $Y_0/D \geqslant 0.47$ (Fig. 4). The flexible cylinder undergoes large-amplitude vibrations over a wide range of reduced velocities and the responses characteristics are very different from that of the isolated cylinder situation. The characteristics of the vibrating response curves change mainly with the lateral separation of the cylinder pair while the influence of the longitudinal separation is less noticeable. At a fixed value of Y_0/D, the response curves observed at different values of X_0/D exhibit similar patterns.

As a typical example, Fig. 11 shows the vibration responses at different lateral separations at the same longitudinal cylinder separation of $X_0/D = 1.41$. Three sub-regions of unique response characteristics can be identified according to the value of Y_0/D. At $Y_0/D = 0.47$, vibration level increases with reduced velocity in an almost monotonic manner.

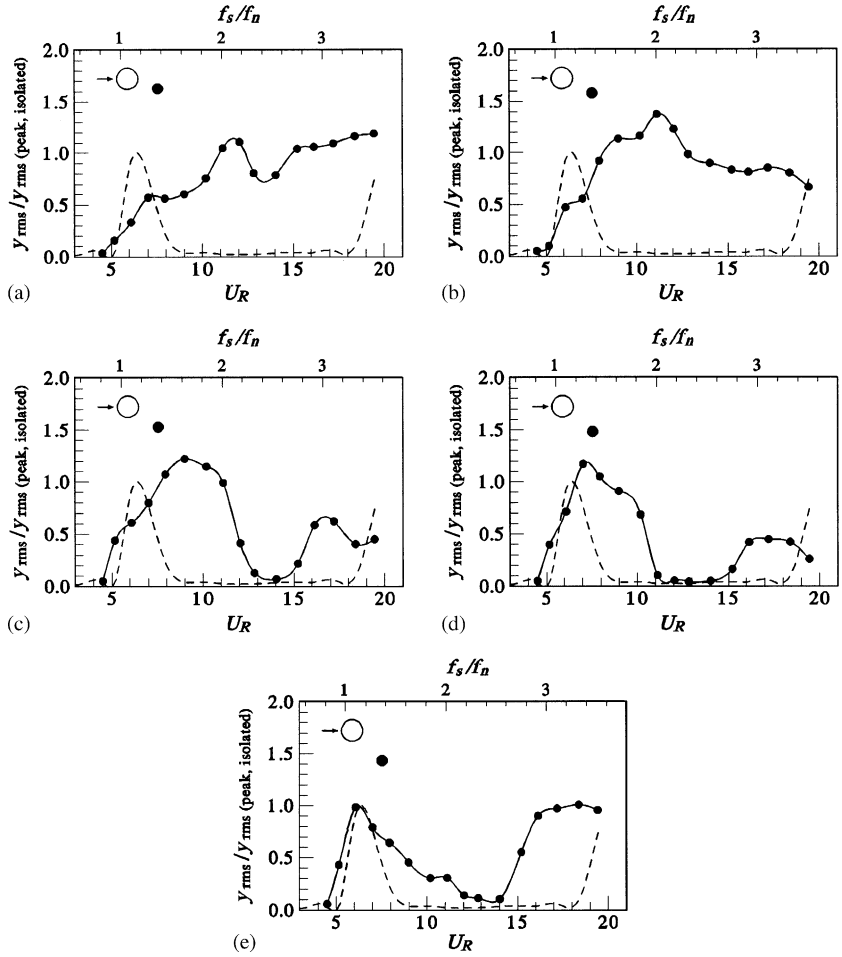

Fig. 11. Vibration response of the smaller cylinder in the staggered arrangement at $X_0/D = 1.41$. Y_0/D: (a) 0.47; (b) 0.70; (c) 0.94; (d) 1.17; (e) 1.41.

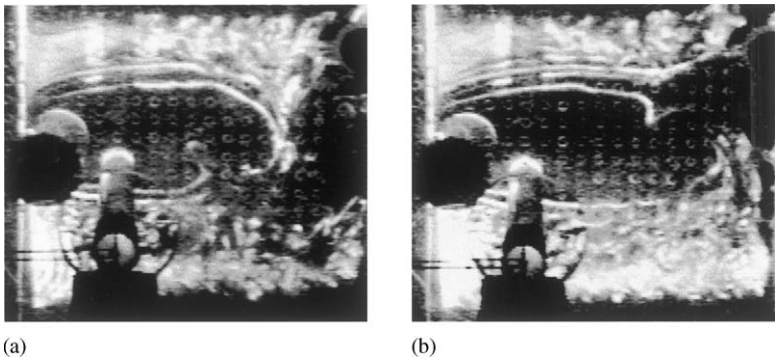

Fig. 12. Phase-locked smoke visualizations in the staggered arrangement. Single body wake at $(X_0/D, Y_0/D) = (0.94, 0.47)$. $U_R = 12.0$. Smaller cylinder at extreme positions: (a) nearest to the larger cylinder; (b) farthest away from the larger cylinder.

This pattern is observed for nearly all longitudinal separations at this value of Y_0/D (Fig. 4). The next sub-region is at $Y_0/D = 0.70$ where high-level vibrations occur over a very wide range of reduced velocity with one main maximum peak in the response curve. This pattern is observed at most of the longitudinal separations shown in Fig. 4. At $Y_0/D \geqslant 0.94$, two separated resonance regions are observed in the response curves and there is a gradual shift of the peak reduced velocity in the first resonance region to lower values as Y_0/D increases. The responses curves do not change much with the change in X_0/D. The flow patterns at these three sub-regions will be discussed in sequence.

3.7. Staggered arrangement: single body wake

At $Y_0/D = 0.47$, Fig. 11a shows that at $U_R > 4$, the vibration amplitude starts to build up in a near-monotonic manner to a peak response at $U_R = 11.5$ after passing through a transient peak at $U_R = 7$. These two values of reduced velocity correspond to frequency ratio values of 2.1 and 1.3, respectively. The resonance is believed to be of the lock-in type. Between $U_R = 13$ and 14, the vibration amplitude drops to a valley and then increases to a constant high level for $U_R > 15$. It was observed during the experiments that the two ends of the flexible cylinder vibrated in an in-phase manner in this last resonance region. The mode of vibration is not of the torsional type but of the coherent type. Fig. 4 shows that at a small longitudinal separation between the cylinders, at $X_0/D = 0.70$ or 0.94, there are only low amplitudes of vibration at reduced velocities below $U_R < 10$ but a small peak near $U_R = 7$ still appears in the response curves.

Fig. 12 shows the flow visualization pictures obtained at $U_R = 12$ when the cylinders are separated at $(X_0/D, Y_0/D) = (0.94, 0.47)$. Smoke pictures have been taken throughout the whole velocity range but the most repeatable flow patterns best phase-locked to the cylinder movements are obtained at this reduced velocity where peak vibration level occurs. The visualizations show that there exists little flow in the gap region between the cylinders, no matter when the smaller cylinder is at either of its extreme positions nearest to or farthest away from the larger cylinder. The smoke-marked flow passes over the two cylinders like a single body.

The smoke streaks show that the shear layer on the free side of the larger cylinder feeds vorticity continuously into an attaching vortex. On the other side, the shear layer from the larger cylinder seems to join to the free side of the smaller cylinder and vorticity is fed to another attaching vortex. When the flexible smaller cylinder reaches its extreme position nearest to the larger cylinder, the separation between the two shear layers becomes the shortest. This facilitates the intrusion of freestream flow into the wake from the smaller cylinder side which leads to the shedding of the vortex from the free side of the larger cylinder (Fig. 12a). Shedding of the other vortex from the smaller cylinder side occurs when the smaller cylinder moves to its other extreme position farthest away from the larger cylinder (Fig. 12b).

The vortices shed from either side have very similar sizes and scales. The vortex shedding pattern as shown in Fig. 12 resembles that occurring behind a single body. Fig. 13 shows an example of the velocity field in the wake at this lateral separation $Y_0/D = 0.47$. Both the mean and r.m.s. axial velocity distributions suggest that flow passes around the two cylinders as if they are a single body. A combined wake is formed behind the cylinders and the width of the wake is about the same as that of the larger cylinder alone. The shedding frequency of the vortices from the two cylinders as a single body scales on the width of this wake. Therefore, the vortex shedding frequency will match the natural frequency f_n of the flexible cylinder near $U_R = 12$, that is a frequency ratio of f_s/f_n at approximately two. The vibration is sustained by the IIE mechanism.

Fig. 14 shows how the vibration spectra and the wake velocity spectra vary with the freestream velocity. The velocity spectra are obtained on the free side of the smaller cylinder side in the combined wake. At all reduced velocities, the flexible cylinder always vibrates at its natural frequency f_n. The vortex shedding frequency as revealed by the peak in the velocity is locked on to f_n between $U_R = 9-13$. As the reduced velocity increases beyond $U_R > 14$, the peak frequency of wake velocity fluctuations increases again linearly with U_R. In this resonance region, the cylinder also undergoes large-amplitude vibrations at frequency f_n. It is believed that this is due to a mechanism similar to "wake galloping". At this particular lateral separation between the two cylinders, the smaller cylinder is located at one side-edge of the larger cylinder wake. Fig. 13, for instance, shows that there exists very low velocity flow over the inner side of the smaller cylinder but the free side is exposed to flow at near the free-stream value. This results in a lift force acting to push the smaller cylinder farther into the larger cylinder wake, at which position the lift force diminishes or even reverses direction. Vibrations of the flexible smaller cylinder can thus be sustained by this fluctuating lifting action in a similar way as a highly flexible cylinder undergoing wake galloping in the side wake of an upstream cylinder.

In the present staggered arrangement of two unequal-sized cylinders at this small lateral separation, flow is not observed in the gap region between the two cylinders. In the situation of two equal-sized cylinders placed in the staggered arrangement with a small lateral separation, significant gap flow has been observed in Zdravkovich and Pridden (1977). Another different observation made in that reference is that the maximum lift force acting on the downstream cylinder is found at a lateral separation at 0.25 cylinder diameter. Bokaian and Geoola (1984) found,

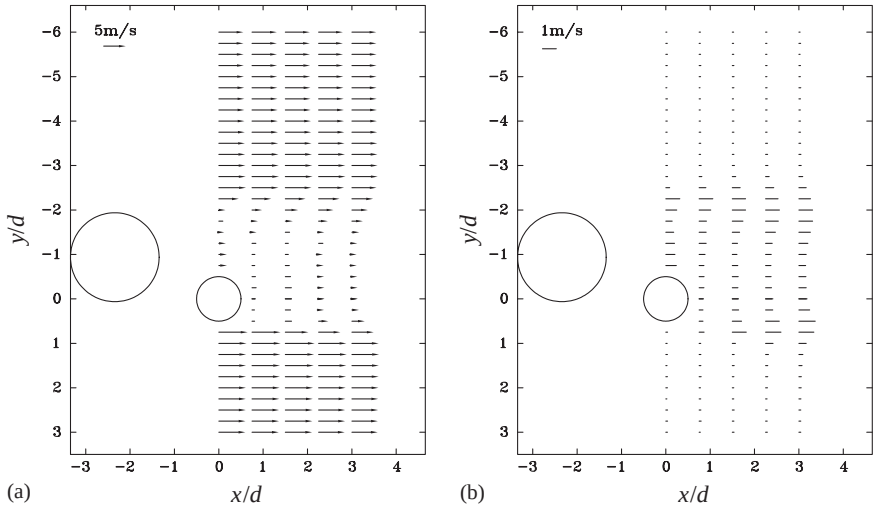

Fig. 13. Distribution of (a) mean axial velocity; and (b) r.m.s. velocity fluctuations in the wake of the two cylinders in the staggered arrangement $(X_0/D, Y_0/D) = (1.17, 0.47)$.

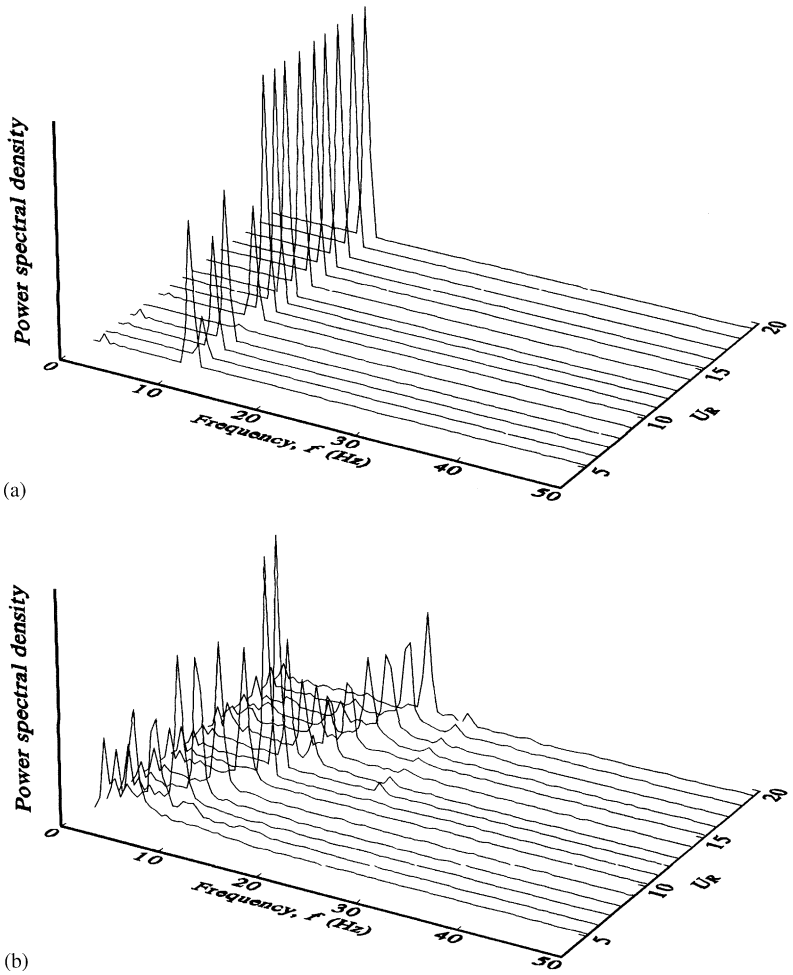

Fig. 14. Vibration and velocity spectra in the staggered arrangement $(X_0/D, Y_0/D) = (1.64, 0.47)$. (a) Vibration spectra of the smaller cylinder; (b) velocity spectra in the wake on the free side of the smaller cylinder.

however, that a maximum lift force occurs at a lateral separation of about 0.5 cylinder diameter when the two equal-sized cylinders are separated longitudinally by a distance of two cylinder diameters. In this study, the particular lateral separation of $0.47D$ or $0.94d$ is found to lead to the maximum lift force on the downstream smaller cylinder. It is not certain of the reasons for these differences in lateral separation for maximum lift force but the Reynolds number seems an important factor. This is because the present experiments and those of Bokaian and Geoola (1984) are performed under similar Reynolds numbers but the experiments of Zdravkovich and Pridden (1977) are made at much higher Reynolds numbers.

In Bokaian and Geoola (1984), peak responses of the downstream flexible cylinder are found at a flow velocity at frequency ratio equal to 1.5. In that situation of two equal-sized cylinders in staggered arrangement, the flow also passes the two cylinders as a single body but the combined wake width is significantly larger than that of a single cylinder and is roughly 1.5 times wider. In the present situation, the presence of the smaller cylinder leads to a combined wake only slightly wider than the larger cylinder wake alone. The resulting wake width, which determines the vortex shedding frequency, is about twice the wake width of the isolated smaller cylinder and the peak response occurs at a freestream velocity corresponding to a frequency ratio roughly at $f_s/f_n = 2$.

3.8. Staggered arrangement: intermittent gap flow

Fig. 4, as well as Fig. 11b, shows that at the lateral separation of $Y_0/D = 0.70$, the response curves of the smaller cylinder cover a very wide range of reduced velocities. Not only are the vibrations occurring more easily at all velocities, the amplitudes of vibration at most reduced velocities also reach levels comparable to or higher than the amplitude of peak lock-in response of the isolated cylinder situation. Flow-induced vibration starts to occur at $U_R = 6$. The vibration amplitude then increases sharply with the reduced velocity reaching a maximum near $U_R = 12$. After a gradual drop in vibration amplitudes between $U_R = 12-14$, another resonance region keeps the vibration amplitude levelling to a plateau at $U_R > 15$. It was observed in the experiments that in this last resonance region, vibrations were of the torsional mode instead of the wake-galloping type as found at the smaller lateral separation of $Y_0/D = 0.47$. Fig. 4 shows that when the longitudinal separation between the cylinders increases, the torsional mode vibration decreases in amplitude.

During the flow visualizations made at this lateral separation, smoke streaks are found intermittently passing through the gap region between the two cylinders. Fig. 15 shows an example of mean axial velocity distribution at $(X_0/D, Y_0/D) = (0.70, 0.70)$. These mean velocity data of long time averaging show the presence of a narrow gap flow of high velocities through the gap between the two cylinders. After passing the smaller cylinder, this gap flow bends sharply towards the larger cylinder. This leads to a time-averaged pattern of a much shortened region of defect velocities behind the larger cylinder but a much wider wake behind the smaller cylinder.

Fig. 16 shows the phase-locked smoke pictures obtained at $U_R = 12$ at which the most repeatable flow patterns are found. When the vibrating smaller cylinder is at its extreme position nearest to the larger cylinder, there is no flow inside the gap region (Fig. 16a). Flow occurs around the two cylinders as a single body. At the other extreme position of the smaller cylinder, the gap region opens up. A smoke streak is visible passing through the gap and is sharply bending into the rear of the larger cylinder (Fig. 16b). At this resonance range, vortices are mainly shed from the two cylinders as a single body and their sizes and frequencies scale essentially as the larger cylinder diameter (Fig. 16). This explains why the peak resonance occurs at $U_R = 12$ where the vortex shedding frequency of the combined body wake matches the natural frequency of the smaller cylinder vibration. However, the presence of the intermittent gap flow provides an additional mechanism to synchronize the instant of vortex shedding with the cylinder movement. The gap flow which is timed by the opening of the gap brings high speed flow into the larger cylinder wake and trigger the shedding of vortices attaching to the free side of the larger cylinder (Fig. 16b). This can explain why the lock-in vibrating amplitude at $U_R = 12$ at this lateral separation $Y_0/D = 0.70$ is the highest among all staggered arrangement positions of the two cylinders (Fig. 4). Different excitation sources of IIE, MIE and EIE are all present and they interact to maximize the vibration levels.

A closer examination of the phase-locked flow pictures between Figs. 16 and 12 reveals that the vortex shedding phases at the present lateral separation are different from those at the smaller lateral separation at $Y_0/D = 0.47$. In both patterns, vortices are shed from the two cylinders as a single body but the phase relations between vortex shedding and cylinder movement are exactly opposite. It is believed that at that smaller lateral separation where no gap flow occurs, the inward movement of the vibrating smaller cylinder shortens the separation distances between the two shear layers and triggers the shedding of a vortex from the free side of the larger cylinder (Fig. 12a). Here in Fig. 16b, shedding of that vortex is triggered by the gap flow which occurs when the smaller cylinder is farthest away from the larger cylinder.

Spectra of the fluctuating wake velocities show the locking of a peak frequency on f_n between $U_R = 10-13$ (To, 1998). At other reduced velocities, lock-on of peak frequency is not observed and the spectra exhibit a broadband distribution.

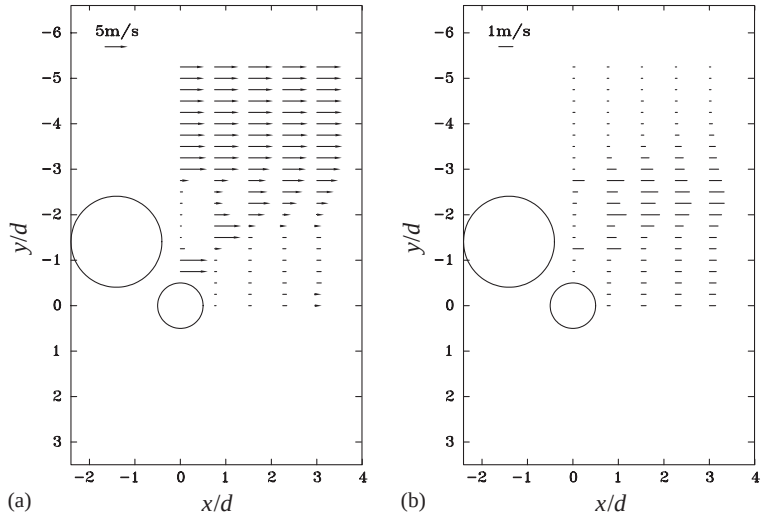

Fig. 15. Distribution of (a) mean axial velocity; and (b) r.m.s. velocity fluctuations in the wake of the two cylinders in the staggered arrangement $(X_0/D, Y_0/D) = (0.70, 0.70)$.

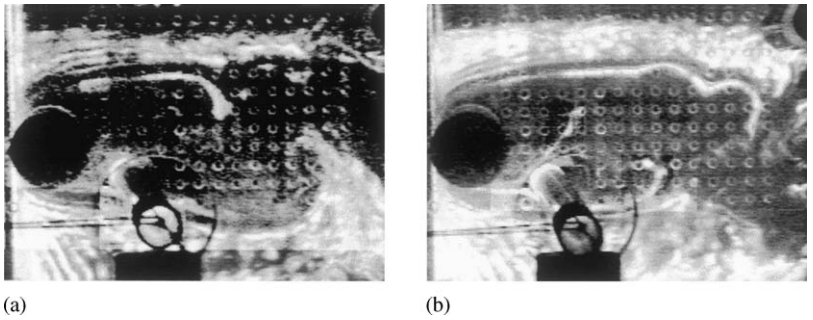

Fig. 16. Phase-locked smoke visualizations in the staggered arrangement. Intermittent gap flow at $(X_0/D, Y_0/D) = (1.17, 0.70)$. $U_R = 12.0$. Smaller cylinder at extreme positions: (a) nearest to the larger cylinder; (b) farthest away from the larger cylinder.

At small longitudinal separations between the cylinders, large-amplitude torsional vibrations occur at $U_R > 15$ and peak responses occur near $U_R = 18$. This resonance range with peak response occurring roughly at the frequency ratio of $f_s/f_n = 3$ has also observed in the flow over two equal-sized cylinders in a similar relative position (Bokaian and Geoola, 1984) but the vibration mode is coherent in that investigation. In the present situation of two unequal-sized cylinders, coherent mode vibrations at this high reduced velocity range are only found at the smaller lateral separation $Y_0/D = 0.47$. This may be due to the smaller damping in the present experiments carried out in a wind tunnel as opposite to the water flume experiments of Bokaian and Geoola (1984). Another factor may be the proximity of the natural frequency of torsional vibration at 12.2 Hz to that of the coherent vibration at 10.5 Hz in the present experiments.

3.9. Staggered arrangement: constant gap flow

When the lateral separation increases beyond $Y_0/D = 0.70$, the response curves at different staggered arrangement positions exhibit a similar shape (Fig. 4). There exists two well-separated resonance regions, one over the reduced velocities between $U_R = 5-12$ and the other between $U_R = 15-19$. The first resonance region should be of the lock-in type and when compared with the lock-in response curve of the isolated cylinder situation, the response cover a broader range of reduced velocities and the peak vibration amplitude occurs at a higher reduced velocity. It is evident in Fig. 11 that with increase in lateral separation, this reduced velocity for peak response exhibits a gradual shift from $U_R = 12$ at $Y_0/D = 0.47$ to lower values, and finally reaching the value $U_R = 6.1$ of the isolated cylinder situation for $Y_0/D \geqslant 1.41$.

In the second resonance region occurring at higher reduced velocities, torsional vibrations were observed in the experiments.

Figs. 17a and b show the smoke pictures at the cylinder separation $(X_0/D, Y_0/D) = (1.17, 0.94)$ phase-locked to the smaller cylinder movement. This highly repeatable patterns are obtained at $U_R = 10.2$ where the peak response occurs. At all positions of the smaller cylinder movements, there always exists some flow in the gap region between the two cylinders. Fig. 17a shows the smoke streak pattern when the smaller cylinder is at its extreme position nearest to the

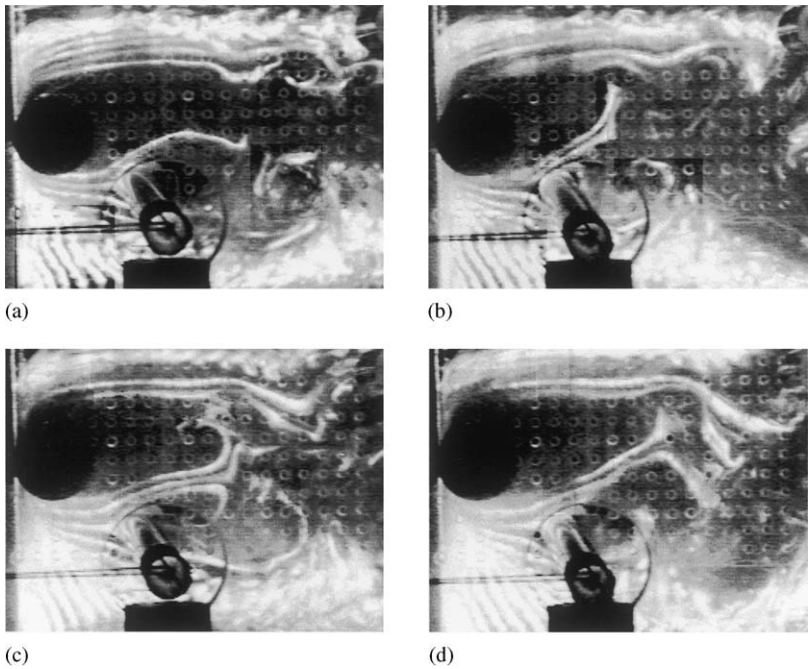

Fig. 17. Phase-locked smoke visualizations in the staggered arrangement. Constant gap flow. (a), (b): $(X_0/D, Y_0/D) = (1.17, 0.94)$. $U_R = 10.2$; (c), (b): $(X_0/D, Y_0/D) = (1.17, 1.17)$. $U_R = 7.9$. Smaller cylinder at extreme positions: (a), (c) nearest to the larger cylinder; (b), (d) farthest away from the larger cylinder.

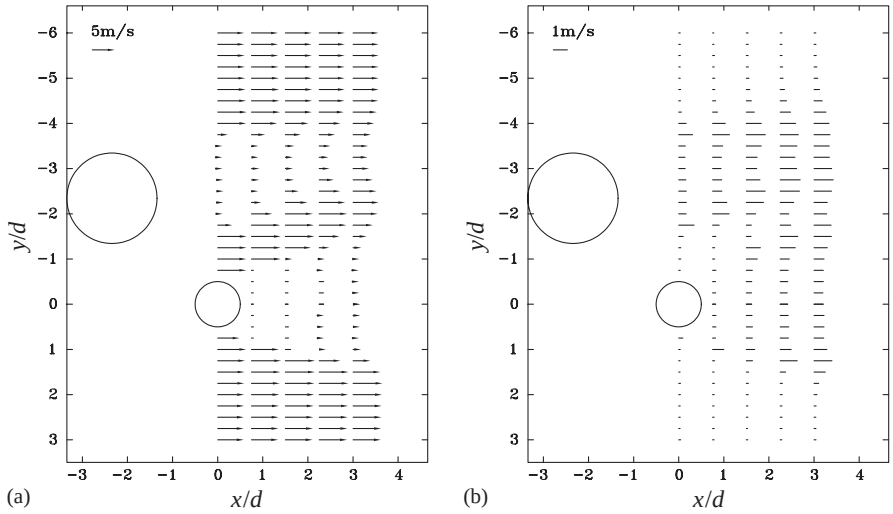

Fig. 18. Distribution of (a) mean axial velocity; and (b) r.m.s. velocity fluctuations in the wake of the two cylinders in the staggered arrangement $(X_0/D, Y_0/D) = (1.17, 1.17)$.

larger cylinder. After passing between the two cylinders, the smoke streaks in the gap region return to a direction near parallel to the freestream. A smoke streak appears to roll up behind the smaller cylinder and a vortex shed from the free side of the smaller cylinder is suggested in Fig. 17a. When the smaller cylinder moves to the other extreme position, the gap flow is bent sharply into the rear of the larger cylinder (Fig. 17b). Similar to Fig. 16, this appears to trigger shedding of a vortex from the free side of the larger cylinder. Figs. 17c and d shows the visualizations at an even wider lateral separation at $Y_0/D = 1.17$. The gap flow is wider and different parts of the smoke streaks in the gap region roll up behind the two cylinders. The movement of the smaller cylinder away from the larger cylinder in Fig. 17d still leads to a bending of the gap flow towards the larger cylinder side but the degree of the effect is smaller than that in Fig. 17b. The smoke pictures in Figs. 17c and d are obtained at the reduced velocity of peak response which is now shifted down to $U_R = 7.9$. When the lateral separation increases to $Y_0/D = 1.41$, the smoke pictures, not shown here, show that there exists wide enough flow in the region between the two cylinders that vortex development occurs on both cylinders themselves (To, 1998). The reduced velocity for peak responses is shifted back to the isolated cylinder value at $U_R = 6.1$.

It is obvious from the smoke pictures in Fig. 17 that an own wake of the smaller cylinder itself can be formed with the constant existence of a gap flow. However, the shape of this smaller cylinder wake is time-varying as affected by the position of the vibrating smaller cylinder. The time-averaged width of the wake may have a width larger than the isolated cylinder situation as a result of gap flow bending towards the larger cylinder side. The wider wake width behind the smaller cylinder is clearly evident from an example of mean velocity distribution shown in Fig. 18. With a wider wake, the vortex shedding frequency at a given velocity becomes lower. This explains why the peak lock-in response occurs at a reduced velocity higher than the isolated cylinder value of $U_R = 6.1$. This widening of smaller cylinder wake is more pronounced at the smaller lateral separations. The peak reduced velocity thus shifts gradually from $U_R \approx 10$ at $Y_0/D = 0.94$, to $U_R \approx 7.5$ at $Y_0/D = 1.17$, and finally to $U_R = 6.1$ at $Y_0/D = 1.41$.

3.10. Flow interaction mechanisms

In all the 64 cylinder arrangement positions except the side-by-side and proximity arrangements, the larger cylinder is placed in a clear upstream position to the smaller cylinder. It is expected that flow incident on the smaller cylinder contains fluctuations arising from the wake of the larger cylinder. If vortex shedding from the larger cylinder and flow-induced vibration of the smaller cylinder can be decoupled, the simple expectation is that at a flow velocity with frequency ratio $f_s/f_n = 2$, large-amplitude vibration of the smaller cylinder will occur due to EIE. This modified lock-in resonance is expected because the larger cylinder vortex shedding frequency at this flow velocity will match the natural frequency of vibration of the smaller cylinder. However, it is found from the investigation that there exists strong interference between the flows around the two cylinders. The modified vibration response of the smaller cylinder exhibits complicated characteristics and is dependent on the relative positions of the two cylinders (Fig. 4). A schematic picture showing some key flow interaction mechanisms in the tandem/near-team and staggered arrangements is presented in Fig. 19.

When the cylinders are placed in the side-by-side arrangement, smoke visualizations show that flow passing through the gap between the two cylinders is always bending towards the rear of the smaller cylinder. This leads to an asymmetric wake behind the cylinder (Fig. 8). A poor periodicity of vortex shedding from the smaller cylinder is reflected in the poor repeatability of smoke patterns phase-locked to the cylinder movement. No vibration is observed at small lateral separations between the cylinders. At larger separations, some vibrations are observed at a reduced velocity lower than the isolated cylinder value of $U_R = 6.1$. This is due to a narrower wake width behind the smaller cylinder as a result of gap flow bending.

In the proximity arrangement when the smaller cylinder is only slightly more downstream than the side-by-side arrangement ($X_0/D = 0.23$), the flow pattern and the vibration responses are similar to those in the side-by-side arrangement at a large lateral separation. At larger longitudinal separation ($X_0/D = 0.47$), the gap flow is parallel or bent towards the larger cylinder side. There is a reasonably well-established wake formed behind the smaller cylinder (Fig. 10). The vibration response curves are similar to that of the isolated cylinder situation but with slightly lower maximum response amplitudes.

In the tandem and near-tandem arrangement, the smaller cylinder is totally immersed in the wake of the larger cylinder. Wake formation and vortex shedding of the larger cylinder are only slightly affected but wake formation cannot occur on the smaller cylinder (Fig. 19a). The flow velocities around the smaller cylinder and thus the fluid forces on it are of low magnitudes. This leads to an almost total suppression of smaller cylinder vibration at all reduced velocities. At larger longitudinal separations where the smaller cylinder becomes free from the vortex formation length of the larger cylinder, some low-amplitude vibration occurs at a flow velocity at $f_s/f_n = 2$ (Fig. 5b).

In all other arrangement positions termed as the staggered arrangement, the vibration responses are generally amplified by the presence of the larger cylinder in the vicinity. Not only are the maximum vibration amplitudes higher,

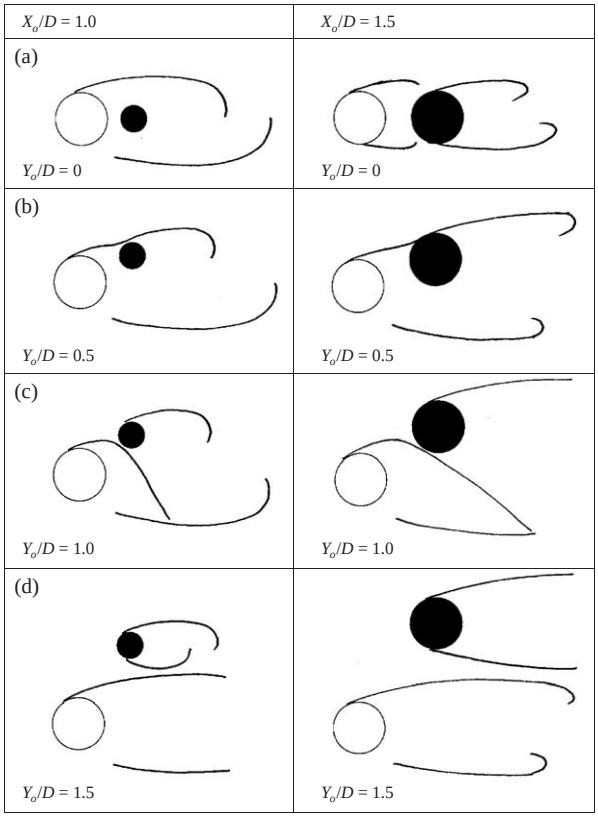

Fig. 19. Schematic diagram showing vortex shedding patterns in different cylinder arrangement positions of two cylinders in the present unequal-sized situation and in the equal-sized situation: (a) tandem; (b) staggered with no gap flow; (c) staggered with intermittent gap flow; (d) staggered with constant gap flow.

large-amplitude vibrations also occur over a broader range of reduced velocities (Fig. 11). The reduced velocity for peak response can have a value between $U_R = 6.1$ ($f_s/f_n = 1$) and $U_R = 12$ ($f_s/f_n = 2$). The vibration response is primarily governed by the lateral separation between the cylinders. This is because the flow features are strongly affected by the absence or presence of an intermittent or consistent gap flow between the cylinders (Fig. 19).

At a small lateral separation, the outer edge of the smaller cylinder is about to be free from the blockage of the upstream larger cylinder (Fig. 19b). Flow is observed to pass the two cylinders as a single body (Fig. 12). The width of the combined wake is about the same size as that of the larger cylinder alone; and so is the vortex shedding frequency. As a result, peak lock-in vibration occurs when the freestream velocity reaches the frequency ratio $f_s/f_n = 2$ ($U_R = 12$). Only low-level vibrations occur at the isolated cylinder value of $U_R = 6$ ($f_s/f_n = 1$).

When the lateral separation between the cylinders increases to about 3/4 the larger cylinder diameter ($Y_o/D = 0.74$), the smaller cylinder is almost completely free from the blockage of the larger cylinder but yet there is no clearance between the projections of the cylinders to the incoming flow (Fig. 19c). Flow essentially passes over the two cylinders as a single body but a gap flow occurs periodically with the movement of the smaller cylinder (Fig. 16). When the smaller cylinder moves to its extreme position farthest away from the larger cylinder, flow passes through the gap which opens between the two cylinders. This triggers vortex shedding from the other side of the larger cylinder. This additional mode of synchronization between cylinder movement and flow excitation source of vortex shedding results in a very high vibration amplitudes at $U_R = 12$ ($f_s/f_n = 2$). Actually, the most severe vibrations of the flexible cylinder, both in terms of vibration amplitudes and width of resonance range of reduced velocity, occur at this lateral separation.

At even larger lateral separations, there is constantly some flow passing through the gap between the two cylinders at all times (Fig. 17). The smaller cylinder starts to develop its own wake which provides the main excitation source for its vibrations (Fig. 19d). The gap flow is still bent towards the larger cylinder side and this leads to a larger width of the smaller cylinder wake as compared to the isolated cylinder situation. The vortex shedding frequency from the smaller cylinder itself is thus lower and peak lock-in occurs at a reduced velocity higher than the isolated cylinder value of $U_R = 6.1$.

The above proposed flow interaction mechanisms are in line with the experiments of Bokaian and Geoola (1984) on two equal-sized cylinders. The flow patterns under different cylinder arrangements are sketched in Fig. 19. In the staggered arrangement, the largest vibration responses are found when the lateral separation between the two cylinders has a value between a half and one diameter distance (Figs. 19b and c). The reduced velocity for peak response is at a frequency ratio larger than one. This is because flow occurs over the two cylinders as a single body. The width of the combined wake is, however, larger than that of one cylinder alone. The vortex shedding frequency at a given velocity is thus lower. When the lateral separation becomes larger than one diameter distance, flow occurs constantly through the gap between the two cylinders (Fig. 19d). Due to the same size of the cylinders, the gap flow is parallel and normal wake development occurs on both cylinders. The vibration responses of the downstream cylinder thus resemble those of an isolated cylinder. When the two cylinders are arranged in tandem, the same-sized upstream cylinder cannot block the flow to the downstream cylinder as in the present situation of a larger cylinder placed upstream (Fig. 19a). Vortex shedding occurs on the downstream cylinder resulting in lock-in vibration.

4. Conclusions

The interference effect of a neighbouring cylinder on the flow-induced vibration response of a flexibly mounted circular cylinder is investigated experimentally. The interfering cylinder is double the size of the vibrating cylinder and is placed upstream of the smaller cylinder. Vibration response curves of the smaller cylinder are obtained at 64 relative arrangement positions of the two cylinders (Fig. 4). Due to flow interaction between the two cylinders, the response curves are more complicated from that of the isolated cylinder situation. Depending on the characteristics of vibration response, the cylinder arrangement positions are classified into different regimes as: tandem/near-tandem, side-by-side, proximity, and staggered. Flow visualizations and wake velocity measurements are carried out to study the flow interaction mechanisms leading to the vibration responses. A number of key flow interaction mechanisms are proposed from the results (Fig. 19).

Flow-induced vibration of the flexible cylinder is greatly suppressed when it is placed side-by-side with the larger cylinder. In the proximity arrangement where the smaller cylinder is more downstream than in the side-by-side arrangement, its vibration response exhibits similar characteristics as those of its isolated situation. In the tandem and near-tandem arrangement, the smaller cylinder is completely sheltered by the larger cylinder. Flow-induced vibration cannot occur at all reduced velocities except $U_R = 12$ at which EIE leads to some low-amplitude lock-in vibration.

In the staggered arrangement, the vibration responses of the smaller cylinder are very different from that of the isolated cylinder situation. Large-amplitude vibrations occur over a broad range of reduced velocities. The amplified responses, in terms of both the vibration amplitudes and reduced velocity ranges, are due to modified lock-in resonance of the smaller cylinder in the presence of the near-by larger cylinder. The lateral separation between the cylinders is found to govern the main features of the vibration response. At small lateral separations, flow occurs over the two cylinders as a single body and a modified lock-in resonance of the smaller cylinder occurs at $U_R = 12$. This is a straightforward case of EIE where the vortex shedding frequency of the combined single body matches the natural frequency of vibration of the flexible smaller cylinder. At large lateral separations at which there is no overlap between the projections of the two cylinders to the flow, flow occurs constantly through the gap between the two cylinders with a possible widening of the wake behind the smaller cylinder. The lock-in resonance thus occurs at a reduced velocity at or higher than the value of $U_R = 6.1$ for the isolated cylinder situation. The most severe vibrations occur when the lateral cylinder separation is about 3/4 the larger cylinder diameter. The smaller cylinder is just about to be free from the shelter of the larger cylinder. An intermittent gap flow occurs periodically with the opening of the gap when the smaller cylinder vibrates in the lateral direction. This leads to the occurrence of the most severe vibrations as a result of the synchronization of the gap flow to the cylinder movements.

A discussion is made on the differences of the present results on two unequal-sized cylinders from the results on two equal-sized cylinders (Bokaian and Geoola, 1984). The flow interaction mechanisms as regard to the gap flow behaviours between the two cylinders are similar but different vibration responses result because of the unequal sizes of the two cylinders.

Acknowledgements

The investigation is supported by a research grant (HKU7007/98E) awarded by the Research Grants Council of Hong Kong.

References

Armstrong, B.J., Barnes, F.H., Grant, I., 1987. A comparison of the structure of the wake behind a circular cylinder in a steady flow with that in a perturbed flow. Physics of Fluids 30, 19–26.

Barbi, C., Favier, D.P., Maresca, C.A., Telionis, D.P., 1986. Vortex shedding and lock-on of a circular cylinder in oscillating flow. Journal of Fluid Mechanics 170, 527–544.

Bearman, P.W., 1984. Vortex shedding from oscillating bluff bodies. Annual Review of Fluid Mechanics 16, 195–222.

Blevins, R.D., 1994. Flow-induced vibrations. Van Nostrand Reinhold Company, New York.

Bokaian, A., Geoola, F., 1984. Wake-induced galloping of two interfering circular cylinders. Journal of Fluid Mechanics 146, 383–415.

Griffin, O.M., Ramberg, S.E., 1976. Vortex shedding from a cylinder vibrating in line with an incident uniform flow. Journal of Fluid Mechanics 75, 257–271.

Griffin, O.M., Hall, M.S., 1995. Vortex shedding lock-on in a circular cylinder wake. In: Bearman, P.W. (Ed.), Flow-Induced Vibrations. A.A. Balkema Press, Rotterdam, pp. 3–25.

King, R., Johns, D.J., 1976. Wake interaction experiments with two flexible circular cylinders in flowing water. Journal of Sound and Vibration 45, 259–283.

Naudascher, E., Rockwell, D., 1994. Flow-Induced Vibrations: an engineering guide. A.A. Balkema Press, Rotterdam.

Ongoren, A., Rockwell, D., 1988. Flow structure from an oscillating cylinder. Part 1. Mechanisms of phase shift and recovery in the near wake. Journal of Fluid Mechanics 191, 197–223.

Sarpkaya, T., 1979. Vortex-induced oscillations—A selective review. Journal of Applied Mechanics 46, 241–258.

Tanida, Y., Okajima, A., Watanabe, Y., 1973. Stability of a circular cylinder oscillating in uniform flow or in a wake. Journal of Fluid Mechanics 61, 769–784.

To, A.P., 1998. Interference effects on the flow-induced vibration of a flexible circular cylinder due to a larger-sized cylinder in the vicinity. Ph.D. thesis, University of Hong Kong, Hong Kong.

Zdravkovich, M.M., Pridden, D.L., 1977. Interference between two circular cylinders; series of unexpected discontinuities. Journal of Industrial Aerodynamics 2, 255–270.

Zhou, Y., Wang, Z.Y., So, R.M.C., Xu, S.J., Jin, W., 2001. Free vibrations of two side-by-side cylinders in a cross flow. Journal of Fluid Mechanics 443, 197–229.